Stretching multistate flexible chains and loops

Geunho Noh [*] and Panayotis Benetatos [†]
Department of Physics, Kyungpook National University, Daegu 41566, Republic of Korea

(Received 13 May 2024; accepted 28 June 2024; published 16 July 2024)

Polymer loop structure commonly appears in biological phenomena, such as DNA looping and DNA denaturation. When a chain forms a loop, its elastic behavior differs from that of an open chain due to the loss of entropy. In the case of reversible loop formation, interesting behavior emerges related to the multistate nature of the conformations. In this study, we model a multistate reversible loop as a looping Gaussian chain, which can bind (close) reversibly at one or several points to form a loop, or a zipping Gaussian loop, which can zip reversibly to form a double-stranded chain. For each model, we calculate the force-extension relations in the fixed-extension (Helmholtz) and the fixed-force (Gibbs) statistical ensembles. Unlike the single Gaussian chain or loop, the multilevel systems demonstrate qualitatively distinct tensile elasticity and ensemble inequivalence. In addition, we investigate a Gaussian necklace consisting of reversible alternating blocks of the zipped chain and loop and obtain the force-temperature phase diagram. The phase diagram implies a force-induced phase transition from a completely looped (denatured) state to a mixed (bound) state.

DOI: 10.1103/PhysRevE.110.014501

I. INTRODUCTION

The elasticity of two-state or multistate soft systems has attracted a lot of interest in recent years because it exhibits unusual features that do not appear in the single-state counterparts of those systems. By multistate systems we mean soft systems whose microstates can be grouped into two or more groups and the macroscopically observed macrostate includes fluctuations between those groups. Many biomolecular systems exhibit such behavior. For example, we can mention polypeptides undergoing helix-coil transitions, DNA chains interacting with DNA-binding proteins that attach and detach reversibly, the reversible unzipping of macromolecular hairpins, the cross-linking of semiflexible bundles, the reversible loop formation in DNA, the formation of denaturation bubbles in double stranded DNA, and the reversible hybridization of oligonucleotides.

A salient feature of two-state or multistate polymers is the statistical ensemble inequivalence for finite-size systems. This is not surprising, as the fluctuations between these states are prominent. Flexible polymers modeled as Gaussian chains are known to exhibit ensemble equivalence as long as the force-extension relation is expressed in terms of conjugate variables (tension and projection of the end-to-end distance on the tension axis) [1–6]. Gaussian chains can exhibit ensemble inequivalence if they are geometrically confined [7–13]. Semiflexibility is another cause of ensemble inequivalence, due to the long-range correlations introduced by the persistence length [14–16].

In this article, we focus on the response of multistate flexible (Gaussian) loops under tension. At first, we consider the single-state case of a loop under tension and we show that effectively it behaves like a single chain. Then we consider three multistate cases: a Gaussian chain that can be open or closed (looped); a Gaussian loop that can be zipped and unzipped in an all-or-none fashion; an infinitely long necklace consisting of concatenated zipped and looped blocks of all sizes.

Loop structures can emerge from a linear polymeric system via conformational changes, a phenomenon commonly observed in biological context such as DNA looping [17–22] and DNA melting [23–32]. These loop formations are reversible processes. For DNA looping, the polymer structure can be either looped state or unlooped state and, for DNA melting, it can be either closed (zipped, double-stranded) state or open (unzipped, bubbled) state. These reversible systems suggest simple scenarios where an open polymer chain can form a closed loop through reversible binding at its end points or a closed polymer loop can zip to form a transient double-stranded chain. As a next step, it is natural to extend the scenarios to include intermediate states where the chain can be partially looped or partially zipped. This motivates a multistate model for the system under consideration.

In the zipping case, the polymer is assumed to undergo all-or-none-like transitions between the unzipped and zipped states. The all-or-none model has long been used to describe aspects of the melting transition of DNA, particularly of oligonucleotides [33–36]. An all-or-none type of zipping is observed in single-molecule kinetic data of oligonucleotide hybridization experiments [37–40], indicative of the validity of the model.

DNA melting can be viewed as a proliferation of denaturation bubbles. In a widely used semimicroscopic approach, double stranded DNA is modeled as a necklace consisting of concatenated blocks of loops (representing the denaturation bubbles) and linear polymers (representing the

[*]Contact author: ngh@knu.ac.kr
[†]Contact author: pben@knu.ac.kr

double-stranded segments). This is the famous Poland-Scheraga model [26] that is usually analyzed using the generating function method [41–46]. An appealing aspect of this model is that it highlights the universal aspects of the phase behavior in the thermodynamic limit. In the original version of the model, the double-stranded segments are modeled as perfectly rigid rods. In order to investigate the effect of reversible bubbles on the elasticity and phase behavior of DNA, variants of the Poland-Scheraga model with the necklace subject to a tensile force have been analyzed [47–50]. In some of these studies [47,48], the zipped part is modeled as a rigid rod, and in Ref. [49] as a freely jointed chain, whereas in Ref. [50] as a semiflexible chain with bending rigidity. In this article, we analyze the Gaussian necklace model, consisting of concatenated reversibly zipping Gaussian loops. It is intended to describe a reversible polymer necklace subject to a small tensile force. The simplicity of this model makes it analytically tractable.

This article is organized as follows. In Sec. II, we review in detail the partition functions of a Gaussian chain and a Gaussian loop and clarify their differences from the corresponding conformational probabilities. In Secs. III and IV, we analyze the tensile elasticity, in both ensembles, of reversible two- or multistate looping Gaussian chains and zipping Gaussian loops. In Sec. V, we consider a flexible necklace under tension whose elements are zipped Gaussian chains and Gaussian loops. We obtain the phase diagram in the force-temperature plane. We summarize and discuss our results in Sec. VI.

II. PARTITION FUNCTION OF THE GAUSSIAN CHAIN AND THE GAUSSIAN LOOP

A. Gaussian chains

Flexible polymers can be described using the Gaussian chain model [51], characterized by the probability density for the end-to-end vector $\boldsymbol{R}$ as $\rho(\boldsymbol{R};N,b)=(3/2\pi)^{3/2}N^{-3/2}\exp(-3\boldsymbol{R}^2/2Nb^2)b^{-3}$. Here, N and b denote the degree of polymerization and the effective bond length of the chain (Kuhn length), respectively. If we fix $\boldsymbol{R}=X\hat{x}+Y\hat{y}+Z\hat{z}$ along a certain direction, say the x axis, and allow fluctuations in the other directions (y-z plane), the y and z components are integrated out, leading to a one-dimensional probability density: $\rho(\boldsymbol{R};N,b)\to\rho(X;N,b)=(3/2\pi)^{1/2}N^{-1/2}\exp(-3X^2/2Nb^2)b^{-1}$. The probability for the end-to-end x projection of the chain being in the small range $[X,X+\Delta X]$ is then $P(X;N,b)=\Delta X\,\rho(X;N,b)$. We refer to the statistical ensemble of the system, described by the distribution $\rho(X;N,b)$ with the extension X, as the control parameter of the measurement, as the fixed-extension ensemble (Helmholtz ensemble), or the X ensemble for brevity.

The partition function for the Gaussian chain in the X ensemble, denoted by $\mathscr{Z}^{\mathrm{H}}$, is proportional to the number of conformational microstates $\Omega(X;N,b)$, since the energy of the Gaussian chain remains constant irrespective of its conformation. In the absence of any external field, we can identify $\mathscr{Z}^{\mathrm{H}}$ with $\Omega(X;N,b)$, which can be obtained by multiplying $P(X;N,b)$ by the number of all possible microstates of the chain with the given N. In order to determine the normalization constant, we employ a random walk on a periodic lattice of ζ neighbors, yielding $\Omega(X;N,b)=\zeta^N P(X;N,b)$ [52]. Consequently, the partition function in the X ensemble is expressed as

$$\mathscr{Z}^{\mathrm{H}}=\left(\frac{3}{2\pi}\right)^{1/2}\sigma\zeta^N N^{-1/2}\exp\left(-\frac{3X^2}{2Nb^2}\right),\tag{1}$$

where $\sigma=\Delta X/b$ is defined as the relative (dimensionless) length scale related to the observation. The average force (tension) in the $\hat{x}$ direction needed to maintain the extension X against the retracting entropic force is given by

$$\langle f\rangle=\frac{\partial F}{\partial X}=\frac{3k_{\mathrm{B}}T}{Nb^2}X,\tag{2}$$

where $F=-k_{\mathrm{B}}T\,\ln\mathscr{Z}^{\mathrm{H}}$ is the Helmholtz free energy and k_{B} is the Boltzmann constant.

In the previous ensemble, the extension X is fixed as the controllable variable, while the force f, conjugate to X, is fluctuating as the responding variable. Let us consider the conjugate ensemble, where the Gaussian chain is subject to a constant tensile force $\pm\boldsymbol{f}=\pm f\hat{x}$ applied to its end points, as the control parameter. We refer to the statistical ensemble corresponding to this physical situation as the fixed-force ensemble (Gibbs ensemble), or the f ensemble for brevity. The partition function for the Gaussian chain in the f ensemble can be expressed as a discrete version of the Laplace transform, $\mathscr{Z}^{\mathrm{G}}=\sum_{\{X\}}\mathscr{Z}^{\mathrm{H}}\exp(fX/k_{\mathrm{B}}T)$, where $\sum_{\{X\}}$ denotes the sum over all intervals $[X,X+\Delta X]$ corresponding to macrostates of X and $\mathscr{Z}^{\mathrm{H}}$ plays the role of the multiplicity of the Boltzmann weight. In the continuum limit of $\sum_{\{X\}}\to\int_{-\infty}^{\infty}dX/\Delta X$, we calculate the partition function in the f ensemble:

$$\mathscr{Z}^{\mathrm{G}}=\zeta^N\exp\left(\frac{Nb^2f^2}{6{k_{\mathrm{B}}}^2T^2}\right).\tag{3}$$

The average extension (end-to-end x projection) of the chain under the tensile force f along the $\pm x$ direction is given by

$$\langle X\rangle=-\frac{\partial G}{\partial f}=\frac{Nb^2}{3k_{\mathrm{B}}T}f,\tag{4}$$

where $G=-k_{\mathrm{B}}T\,\ln\mathscr{Z}^{\mathrm{G}}$ is the Gibbs free energy. This relation can also be obtained from the freely jointed chain for small forces as the linear approximation of $\langle X\rangle=Nb\mathcal{L}(bf/k_{\mathrm{B}}T)\approx Nb^2f/3k_{\mathrm{B}}T$, where $\mathcal{L}$ is the Langevin function [53]. Note that if we just interchange the roles of two conjugate variables, i.e., inverse the control (fixed) and the fluctuating (averaged) variables, Eq. (4) turns to Eq. (2) and vice versa. This demonstrates the ensemble equivalence between the X ensemble and the f ensemble for the Gaussian chain.

What we presented in this subsection is all well known, except for a subtle point. Quite often, the X-partition function and the corresponding conformational probability density are used interchangeably, because they differ by a constant prefactor. This difference is considered irrelevant, because we usually take derivatives of the logarithm of the partition function. However, this is not always the case. As we shall show in the following sections, in two- or multistate systems, such a partition function appears as a term in a sum with other

partition functions having different prefactors. Then, the prefactors affect the thermodynamic observables of the system. The same is true for the kinetic energy part of the partition function that we ignore, assuming massless polymers.

B. Gaussian loops

A Gaussian chain with degree of polymerization N is usually represented by a concatenated chain of N harmonic oscillators, each having an entropic spring constant equal to $3k_BT/b^2$ [51]. The mechanical analogy to N springs in series provides an intuitive way to understand the force-extension relation in Eq. (2) with the spring constant $3k_BT/Nb^2$. The loop structure serves as the most straightforward parallel version of the Gaussian chain and a similar analogy is expected to hold in this context. Let us consider two Gaussian chains of degree of polymerization N_1 and N_2, represented by end-to-end vectors $\boldsymbol{R}_1$ and $\boldsymbol{R}_2$, respectively, each with one of its ends located at the origin. The loop formation can be realized by introducing a step function as a confining potential in a small volume $v \ll b^3$ within which $\boldsymbol{R}_1$ and $\boldsymbol{R}_2$ converge [54]. Using this method of constructing a loop, we can well define the end-to-end vector of the loop as $\boldsymbol{R} = \boldsymbol{R}_1 = \boldsymbol{R}_2$.

The probability density for the end-to-end x-projection X $(= X_1 = X_2)$ of the Gaussian loop can be written by using the delta function as

$$\rho_{\mathcal{O}}(X;N_1,N_2,b) = \int dY_1 \int dZ_1 \int d^3R_2 \rho(\boldsymbol{R}_1;N_1,b) \times \rho(\boldsymbol{R}_2;N_2,b) v\delta(\boldsymbol{R}_1-\boldsymbol{R}_2).$$

The probability for the extension X of the loop being in the small interval $[X, X+\Delta X]$ is $P_{\mathcal{O}}(X;N_1,N_2,b) = \Delta X \rho_{\mathcal{O}}(X;N_1,N_2,b)$ and the corresponding number of conformational microstates is $\Omega_{\mathcal{O}}(X;N_1,N_2,b) = \zeta^{N_1+N_2} P_{\mathcal{O}}(X;N_1,N_2,b)$. As this multiplicity is identical with the partition function of the Gaussian loop in the X ensemble, we obtain the partition function:

$$\mathcal{Z}_{\mathcal{O}}^{\mathrm{H}} = \left(\frac{3}{2\pi}\right)^2 \sigma\tau\zeta^{N_1+N_2}(N_1N_2)^{-1/2}(N_1+N_2)^{-1} \times \exp\left(-\frac{3(N_1+N_2)X^2}{2N_1N_2b^2}\right), \tag{5}$$

where $\tau = v/b^3$ is defined as the relative (dimensionless) range of the looping interaction. The Helmholtz free energy of the Gaussian loop is then $F_{\mathcal{O}} = -k_BT \ln \mathcal{Z}_{\mathcal{O}}^{\mathrm{H}}$ and the force-extension relation in the X ensemble is given by

$$\langle f \rangle = \frac{\partial F_{\mathcal{O}}}{\partial X} = \frac{3(N_1+N_2)k_BT}{N_1N_2b^2}X. \tag{6}$$

In the conjugate scenario, the Gaussian loop is subject to a constant tensile force $\pm\boldsymbol{f} = \pm f\hat{x}$, applied to the end at the origin and to the other end confined within the volume v. Similarly to the previous Sec. II A, the partition function in this f ensemble is written as $\mathcal{Z}_{\mathcal{O}}^{\mathrm{G}} = \sum_{\{X\}} \mathcal{Z}_{\mathcal{O}}^{\mathrm{H}} \exp(fX/k_BT)$. We transform the sum into an integral in the continuum limit

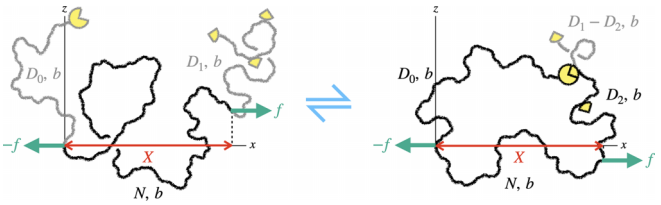

FIG. 1. Model diagram of the reversibly looping Gaussian chain, depicting the four-state case in particular. The left side illustrates the unlooped state and the right side illustrates one of the three possible looped states. The yellow pizzalike shapes represent the binding sites, where the loop is formed. X and $\pm f$ are the control parameters in the extension ensemble and the force ensemble, respectively. This is meant to be a 3D diagram with the y-axis perpendicularly into the page.

and calculate the partition function:

$$\mathcal{Z}_{\mathcal{O}}^{\mathrm{G}} = \left(\frac{3}{2\pi}\right)^{3/2} \tau\zeta^{N_1+N_2}(N_1+N_2)^{-3/2} \times \exp\left(\frac{N_1N_2b^2f^2}{6(N_1+N_2)k_B{}^2T^2}\right). \tag{7}$$

The Gibbs free energy of the Gaussian loop is then $G_{\mathcal{O}} = -k_BT \ln \mathcal{Z}_{\mathcal{O}}^{\mathrm{G}}$ and the force-extension relation in the f ensemble is given by

$$\langle X \rangle = -\frac{\partial G_{\mathcal{O}}}{\partial f} = \frac{N_1N_2b^2}{3(N_1+N_2)k_BT}f. \tag{8}$$

From Eq. (6) and Eq. (8), we confirm, not surprisingly, that the Gaussian loop also exhibits the ensemble equivalence. We also note that the force-extension relation of the loop is exactly that of two springs connected in parallel, with spring constants corresponding to the entropic spring constants of the two Gaussian chains which form the loop.

III. LOOPING GAUSSIAN CHAINS

A. Model

The looping Gaussian chain (ℓGC) consists of a central GC and two dangling GCs connected to its end points, as illustrated in Fig. 1. Although this structure may seem rather peculiar at first glance, constructing the model in this way allows the looping interaction to be made independent of stretching, enabling a straightforward analysis of the tensile elasticity in both the X and f ensembles as affected by the structural changes. The dangling ends fold and connect reversibly to form the loop. Each component consists of degree of polymerization N, D_0, and D_1, represented by position vector $\boldsymbol{R}$, $\boldsymbol{r}_0$, and $\boldsymbol{r}_1$, respectively, with the same Kuhn length b. At the free end of each dangling chain, there is a specific site capable of binding with each other, forming a reversible loop. The looping interaction is governed by a confining potential $V(|\boldsymbol{r}_0 - \boldsymbol{r}_1|)$ defined as

$$V(|\boldsymbol{r}_0-\boldsymbol{r}_1|) = \begin{cases} \varepsilon_v < 0, & \boldsymbol{r}_0 \text{ and } \boldsymbol{r}_1 \text{ within } v, \\ 0, & \text{otherwise.} \end{cases} \tag{9}$$

When it remains an open (unlooped) chain, it is referred to as being in the u state. Conversely, when the ℓGC forms a closed

loop, it is referred to as being in the ℓ state. Building upon this simplest two-state framework, it would be natural to expand the model by incorporating additional binding sites. In fact, looping of DNA often involves a sliding cross-linker [21]. A first step towards modeling this situation would be to consider a sequence of closely spaced binding sites. In order to capture the primary changes in patterns with an increasing number of binding sites, we assume several binding sites exclusively on the dangling chain of D_1 and explore the ℓGC up to the four-state case.

B. Extension ensemble

In the X ensemble for the ℓGC, determining its extension is a necessary first step. We define the end-to-end vector of the ℓGC as $\boldsymbol{R}$ of the central chain. The end-to-end x projection X of the ℓGC is then the x component of $\boldsymbol{R}$. Let us first consider the simplest two-state system. We write the partition function for the two-state ℓGC as

$$\begin{aligned}\mathcal{Z}^{\mathrm{H}}_{\ell\mathrm{GC}} &= \sum_{\{\boldsymbol{r}_0,\boldsymbol{r}_1\in v\}} \exp\left(-\frac{\varepsilon_v}{k_{\mathrm{B}}T}\right) + \sum_{\{\boldsymbol{r}_0,\boldsymbol{r}_1\notin v\}} \exp(0)\\ &= \mathcal{Z}^{\mathrm{H}}_{\mathcal{O}} \exp\left(-\frac{\varepsilon_v}{k_{\mathrm{B}}T}\right) + \left(\mathcal{Z}^{\mathrm{H}}_{\ell\mathrm{GC,u}} - \mathcal{Z}^{\mathrm{H}}_{\mathcal{O}}\right)\\ &= \mathcal{Z}^{\mathrm{H}}_{\ell\mathrm{GC,u}} + \mathcal{Z}^{\mathrm{H}}_{\mathcal{O}}\left[\exp\left(-\frac{\varepsilon_v}{k_{\mathrm{B}}T}\right) - 1\right], \end{aligned} \tag{10}$$

where $\mathcal{Z}^{\mathrm{H}}_{\ell\mathrm{GC,u}}$ denotes the partition function for the u state in the X ensemble. From the previous results in Sec. II, we directly obtain it as

$$\begin{aligned}\mathcal{Z}^{\mathrm{H}}_{\ell\mathrm{GC,u}} &= \zeta^{D_0}\mathcal{Z}^{\mathrm{H}}\zeta^{D_1}\\ &= \left(\frac{3}{2\pi}\right)^{1/2}\sigma\zeta^{N+D_0+D_1}N^{-1/2}\exp\left(-\frac{3X^2}{2Nb^2}\right). \end{aligned} \tag{11}$$

From Eq. (10), the partition function for the ℓ state is given by

$$\mathcal{Z}^{\mathrm{H}}_{\ell\mathrm{GC},\ell} = \mathcal{Z}^{\mathrm{H}}_{\mathcal{O}} \exp\left(\frac{\varepsilon}{k_{\mathrm{B}}T}\right), \tag{12}$$

where ε is a phenomenological energy parameter defined as

$$\exp\left(\frac{\varepsilon}{k_{\mathrm{B}}T}\right) = \exp\left(-\frac{\varepsilon_v}{k_{\mathrm{B}}T}\right) - 1. \tag{13}$$

Note that the value of ε can be positive or negative depending on the depth of the confining potential well $|\varepsilon_v|$.

We can directly obtain $\mathcal{Z}^{\mathrm{H}}_{\ell\mathrm{GC},\ell}$ from the result for the Gaussian loop [Eq. (5)] by making the replacement $N_1 = N$ and $N_2 = D_0 + D_1$. Nevertheless, we present a derivation starting from finding the probability density to maintain the consistency in the process. The probability density for $\boldsymbol{r}_0$ and $\boldsymbol{r}_1$ follow Gaussian distributions as $\boldsymbol{r}_0$ represents the end-to-end vector of the Gaussian chain of D_0 and the distribution for $\boldsymbol{r}_1$ mirrors that of the end-to-end vector $\boldsymbol{r}_1 - \boldsymbol{R}$ of the Gaussian chain of D_1. With knowledge of all the relevant distributions for $\boldsymbol{R}$, $\boldsymbol{r}_0$, and $\boldsymbol{r}_1$, the probability density for X of the ℓGC in the ℓ state is obtained by integrating out all the fluctuating components, considering $\boldsymbol{r}_0$ and $\boldsymbol{r}_1$ confined within the volume element $v \ll b^3$. By using the delta function, we write down this scheme as

$$\begin{aligned}\rho_\ell(X;N,D_0,D_1,b) = \int dY \int dZ \int d^3r_0 \int d^3r_1\\ \times\ \rho(\boldsymbol{R};N,b)\rho(\boldsymbol{r}_0;D_0,b)\\ \times\ \rho(\boldsymbol{r}_1-\boldsymbol{R};D_1,b)v\delta(\boldsymbol{r}_0-\boldsymbol{r}_1).\end{aligned}$$

Just as shown in Sec. II, we determine the corresponding probability by introducing ΔX and the resulting number of conformational microstates by employing the random walk of ζ neighbors. Taking into account the looping energy parametrized by ε for the ℓ state, we calculate the partition function in Eq. (12) as

$$\begin{aligned}\mathcal{Z}^{\mathrm{H}}_{\ell\mathrm{GC},\ell} &= \zeta^{N+D_0+D_1}\Delta X\,\rho_\ell(X;N,D_0,D_1,b)\exp\left(\frac{\varepsilon}{k_{\mathrm{B}}T}\right)\\ &= \left(\frac{3}{2\pi}\right)^2\sigma\tau\zeta^{N+D_0+D_1}[N(D_0+D_1)]^{-1/2}\\ &\quad\times\ (N+D_0+D_1)^{-1}\\ &\quad\times\ \exp\left(-\frac{3(N+D_0+D_1)X^2}{2N(D_0+D_1)b^2}+\frac{\varepsilon}{k_{\mathrm{B}}T}\right), \end{aligned} \tag{14}$$

where, as a reminder, $\sigma = \Delta X/b$ and $\tau = v/b^3$. As expected, the obtained result is essentially the same as the one for the Gaussian loop [Eq. (5)], apart from the new factor ε.

The total partition function $\mathcal{Z}^{\mathrm{H}}_{\ell\mathrm{GC}}$ in Eq. (10) is the sum of individual partition functions in Eq. (11) and Eq. (14). The Helmholtz free energy of the system is $F_{\ell\mathrm{GC}} = -k_{\mathrm{B}}T\ \ln\mathcal{Z}^{\mathrm{H}}_{\ell\mathrm{GC}}$ and the force-extension relation is given by $\langle f\rangle = \partial F_{\ell\mathrm{GC}}/\partial X$. In a dimensionless form, it is expressed as

$$\left\langle\frac{f}{k_{\mathrm{B}}T/b}\right\rangle = 3\left(P^{\mathrm{H}}_{\ell\mathrm{GC},u} + \frac{N+D_0+D_1}{D_0+D_1}P^{\mathrm{H}}_{\ell\mathrm{GC},\ell}\right)\frac{X}{L}, \tag{15}$$

where $L = Nb$ is the total contour length of the central chain and $P^{\mathrm{H}}_{\ell\mathrm{GC},i} = \mathcal{Z}^{\mathrm{H}}_{\ell\mathrm{GC},i}/\mathcal{Z}^{\mathrm{H}}_{\ell\mathrm{GC}}$ is the probability of being in the i state ($i = \mathrm{u}, \ell$) in the X ensemble. Note that, if either probability becomes zero, the force-extension relation reverts to the previous results: the one for the single Gaussian chain [Eq. (2)] when $P^{\mathrm{H}}_{\ell\mathrm{GC},\ell} = 0$ or the single Gaussian loop [Eq. (6)] when $P^{\mathrm{H}}_{\ell\mathrm{GC},u} = 0$.

Next, let us consider the multistate ℓGC where the attachment of the end point $\boldsymbol{r}_0$ of the one dangling chain is not restricted to a single binding site on the other end point $\boldsymbol{r}_1$. Instead, it has freedom to bind to several binding sites, providing multiple options for its looping states. We refer to these various looped states as ℓ_i state ($i = 1, 2, 3, \ldots$), where the ℓ_1 state corresponds to the ℓ state in the two-state system. In an intermediate ℓ_i state ($i \neq 1$), D_i monomers engage in forming the loop structure, while the remaining $D_1 - D_i$ monomers form a dangling chain. Accordingly, the partition function for the ℓ_i state in the X ensemble is collectively expressed as

$$\begin{aligned}\mathcal{Z}^{\mathrm{H}}_{\ell\mathrm{GC},\ell_i} &= \left(\frac{3}{2\pi}\right)^2\sigma\tau\zeta^{N+D_0+D_1}[N(D_0+D_i)]^{-1/2}\\ &\quad\times\ (N+D_0+D_i)^{-1}\\ &\quad\times\ \exp\left(-\frac{3(N+D_0+D_i)X^2}{2N(D_0+D_i)b^2}+\frac{\varepsilon}{k_{\mathrm{B}}T}\right). \end{aligned} \tag{16}$$

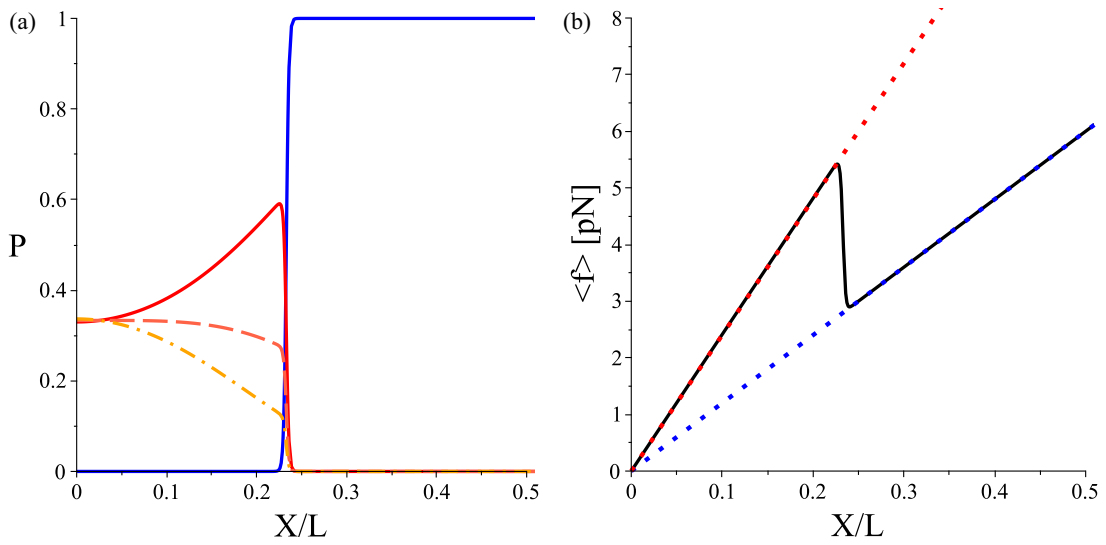

FIG. 2. (a) Probabilities (occurrence frequencies) for each state of the four-state ℓGC in the X ensemble. The red curves correspond to the three looped states: the solid one to the loop consisting of $N + D_0 + D_1$ monomers, the dashed one to $N + D_0 + D_2$, and the dash-dotted one to $N + D_0 + D_3$. The blue curve corresponds to the unlooped state. (b) The force-extension relation of the four-state ℓGC in the X ensemble. The dotted lines serve as visual reference, with the red one representing the relation for a single Gaussian loop consisting of $N + D_0 + D_1$ monomers and the blue one for the single Gaussian chain of N monomers.

In general, the partition function for the m-state ℓGC ($m = 2, 3, 4, \ldots$) in the X ensemble is $\mathscr{Z}^{\rm H}_{\ell{\rm GC}} = \mathscr{Z}^{\rm H}_{\ell{\rm GC,u}} + \sum_{i=1}^{m-1} \mathscr{Z}^{\rm H}_{\ell{\rm GC},\ell_i}$ and the Helmholtz free energy is $F_{\ell{\rm GC}} = -k_{\rm B}T \ln \mathscr{Z}^{\rm H}_{\ell{\rm GC}}$. The force extension relation of the m-state ℓGC in the X ensemble is given by

$$\left\langle \frac{f}{k_{\rm B}T/b} \right\rangle = 3\left(P^{\rm H}_{\ell{\rm GC},u} + \sum_{i=1}^{m-1} \frac{N + D_0 + D_i}{D_0 + D_i} P^{\rm H}_{\ell{\rm GC},\ell_i} \right) \frac{X}{L}, \quad (17)$$

where $P^{\rm H}_{\ell{\rm GC},\ell_i} = \mathscr{Z}^{\rm H}_{\ell{\rm GC},\ell_i}/\mathscr{Z}^{\rm H}_{\ell{\rm GC}}$ is the probability of being in the ℓ_i state in the X ensemble. Figure 2 illustrates the equilibrium statistics and tensile elasticity of the multistate ℓGC with the four-state case (unlooped plus three looped states). Figure 2(a) shows the probability for each state and Fig. 2(b) shows the resulting force-extension relation. In our model, we set $T = 300$ K (corresponding to $k_{\rm B}T \approx 4$ pN nm) and $\tau = (0.1)^3$. We assume a set of sufficiently large numbers of monomers for macromolecules: $(N, D_0, D_1, D_2, D_3) = (1000, 500, 500, 490, 480)$ and a modest value of the Kuhn length for typical synthetic polymers: $b = 10$ Å. Considering a noncovalent type (~10 kcal/mol) of looping interaction, we use $\varepsilon = 100 k_{\rm B}T$ (corresponding to $\varepsilon_v \approx -60$ kcal/mol). The values of σ and ζ turn out to be irrelevant to the results, as they cancel out in the form of probability. The probability pattern exhibits a clear distinction between a small extension regime where the looped states dominate and a large extension regime where the unlooped state dominates. This is reflected in the force-extension relation, resulting in a noticeable crossover between the looped states with the higher stiffness and the unlooped state with the lower stiffness. The crossover regime can be approximately determined by setting the probability of being in the unlooped state to 1/2, as it transitions from near 0 to near 1. In this way, we can characterize the transition in terms of the applied extension $X_{\rm t}$ in the X ensemble. In general, the probability is written as

$$P^{\rm H}_{\ell{\rm GC},u} = \left\{ 1 + \sum_{i=1}^{m-1} \left(\frac{3}{2\pi}\right)^{3/2} \tau (D_0 + D_i)^{-1/2} (N + D_0 + D_i)^{-1} \times \exp\left[-\frac{3N^2}{2(D_0 + D_i)} \left(\frac{X}{L}\right)^2 + \frac{\varepsilon}{k_{\rm B}T} \right] \right\}^{-1}. \quad (18)$$

For our illustration of the $m = 4$ case with the parameter values mentioned above, the equation $P^{\rm H}_{\ell{\rm GC},u}(X_{\rm t}) = 1/2$ yields a numerical value $(X_{\rm t}/L) \approx 0.233$. For the simplest case of $m = 2$, $X_{\rm t}$ is generally expressed as

$$\left(\frac{X_{\rm t}}{L}\right)_{2\text{-}\ell{\rm GC}} = \left\{ \frac{2(D_0 + D_1)}{3N^2} \left[\frac{3}{2} \ln\left(\frac{3}{2\pi}\right) + \ln \tau + \ln\left(\frac{\sqrt{D_0 + D_1}}{(D_0 + D_1)(N + D_0 + D_1)} \right) + \frac{\varepsilon}{k_{\rm B}T} \right] \right\}^{1/2}. \quad (19)$$

Here, the existence of $X_{\rm t}$ depends on the choice of parameter values, in accordance with $0 < X_{\rm t}/L < 1$.

In the crossover regime, it is interesting to observe that the system exhibits negative extensibility (the negative slope). This implies an instability, where the strength of elongational force needed to maintain the size of the chain decreases as the extension increases. Something similar happens when we plot the pressure-volume van der Waals equation of state for $T < T_{\rm c}$. In that case, the instability (negative compressibility) is unphysical and is lifted by means of the Maxwell construction (equal area rule) [55]. However, the case of multistate (multistable) systems is different. As explained by Skvortsov *et al.* in Ref. [10], the van der Waals gas is described by a local order parameter and phase separation occurs, whereas

multistate systems such as ours are described by a global order parameter.

Let us now investigate how the tensile elastic behavior changes with some variations in the parameters of the system. The force-extension relation converges towards the relation for the single Gaussian chain in the case of decreasing $\varepsilon \to -\infty$ (corresponding to $\varepsilon_v \to 0$, i.e., no energy difference between the outside and inside of the confining volume v) or the single Gaussian loop in the case of increasing $\varepsilon \to \infty$ (corresponding to $\varepsilon_v \to -\infty$, i.e., the confining volume v becomes infinite potential well). As the value of τ (range of binding interaction) decreases or increases, the transition regime shifts to the left or right, with its slope becoming smoother or steeper. Since τ determines the effective range of looping interaction, its value affects the frequency of looping events. With a shorter interaction range, it is relatively less likely to be in the looped state, given X/L. Also, as the looping interaction range τ decreases, the width of the negative extensibility regime increases, resulting in the crossover occurring in a less jumplike manner. As the separation between the intermediate binding sites ($D_1 - D_2$ and $D_2 - D_3$) increases, the force-extension curve in the looped state regime deviates from the simple linear response, characteristic of the single loop. This deviation can be attributed to the system undergoing more abrupt changes in the stiffness, as it moves through more distinct looped states. Similar behavior to the four-state ℓGC is observed in the two- or three-state case, revealing no qualitative difference.

C. Force ensemble

In a similar way to Eq. (11), we obtain the partition function for the u state in the f ensemble

$$\begin{aligned}\mathscr{Z}^{\mathrm{G}}_{\ell\mathrm{GC,u}} &= \zeta^{D_0}\,\mathscr{Z}^{\mathrm{G}}\zeta^{D_1} \\ &= \zeta^{N+D_0+D_1}\exp\left(\frac{Nb^2f^2}{6{k_\mathrm{B}}^2T^2}\right).\end{aligned} \tag{20}$$

From Eq. (16), we also directly obtain the partition function for the ℓ_i state in the f ensemble

$$\begin{aligned}\mathscr{Z}^{\mathrm{G}}_{\ell\mathrm{GC},\ell_i} &= \sum_{\{X\}}\mathscr{Z}^{\mathrm{H}}_{\ell\mathrm{GC},\ell_i}\exp\left(\frac{fX}{k_\mathrm{B}T}\right) \\ &= \left(\frac{3}{2\pi}\right)^{3/2}\tau\zeta^{N+D_0+D_1}(N+D_0+D_i)^{-3/2} \\ &\quad\times\exp\left(\frac{N(D_0+D_i)b^2f^2}{6(N+D_0+D_i){k_\mathrm{B}}^2T^2}+\frac{\varepsilon}{k_\mathrm{B}T}\right).\end{aligned} \tag{21}$$

Following a similar process as in deriving Eq. (17), the force-extension relation of the m-state ℓGC in the f ensemble is calculated by differentiating the Gibbs free energy $G_{\ell\mathrm{GC}} = -k_\mathrm{B}T\,\ln\mathscr{Z}^{\mathrm{G}}_{\ell\mathrm{GC}}$ with respect to f. In a dimensionless form, it is expressed as

$$\left\langle\frac{X}{L}\right\rangle = \frac{1}{3}\left(P^{\mathrm{G}}_{\ell\mathrm{GC},u}+\sum_{i=1}^{m-1}\frac{D_0+D_i}{N+D_0+D_i}P^{\mathrm{G}}_{\ell\mathrm{GC},\ell_i}\right)\frac{f}{k_\mathrm{B}T/b}, \tag{22}$$

where $P^{\mathrm{G}}_{\ell\mathrm{GC,u}}$ and $P^{\mathrm{G}}_{\ell\mathrm{GC},\ell_i}$ are the probabilities for each state in the f ensemble. Figure 3 illustrates the probabilities [Fig. 3(a)] and the resulting force-extension relation [Fig. 3(b)] for the four-state ℓGC. Here, the same parameter values are used for consistency between the X ensemble. As seen in the X ensemble, there is a crossover between the looped state regime and the unlooped state regime. The applied force f_t at which the crossover (transition) occurs can be approximately obtained from the equation $P^{\mathrm{G}}_{\ell\mathrm{GC},u}(f_\mathrm{t}) = 1/2$, for given values of the other parameters. The general expression of the probability is

$$\begin{aligned}P^{\mathrm{G}}_{\ell\mathrm{GC},u} = \Bigg\{1+\sum_{m=1}^{m-1}\left(\frac{3}{2\pi}\right)^{3/2}\tau(N+D_0+D_i)^{-3/2} \\ \times\exp\left[-\frac{N^2}{6(N+D_0+D_i)}\left(\frac{f}{k_\mathrm{B}T/b}\right)^2+\frac{\varepsilon}{k_\mathrm{B}T}\right]\Bigg\}^{-1}.\end{aligned} \tag{23}$$

For our $m = 4$ case, we obtain $f_\mathrm{t} \approx 3.952$ pN. In the simpler case of $m = 2$, we obtain a closed analytic expression,

$$\begin{aligned}\left(\frac{f_\mathrm{t}}{k_\mathrm{B}T/b}\right)_{2\text{-}\ell\mathrm{GC}} = \Bigg\{\frac{6(N+D_0+D_1)}{N^2}\Bigg[\frac{3}{2}\ln\left(\frac{3}{2\pi}\right)+\ln\tau \\ -\frac{3}{2}\ln(N+D_0+D_1)+\frac{\varepsilon}{k_\mathrm{B}T}\Bigg]\Bigg\}^{1/2}.\end{aligned} \tag{24}$$

Here, the existence of f_t depends on the choice of the parameter values, in accordance with $0 < \langle X/L\rangle(f_\mathrm{t}) < 1$.

In both cases of X and f ensembles, the ℓGC undergoes a crossover from the looped state to the unlooped state with increasing the corresponding control parameter of stretching (extension or force). In the f ensemble, however, the slope of the force-extension curve, now representing the compliance (the inverse of the stiffness), is always positive. In other words, the negative stiffness in the crossover regime (measured in the X ensemble) does not invert itself to become the negative compliance (measured in the f ensemble). We see that, among the conjugate pair of variables comprising the Hamiltonian of a given system, the choice of which variable to consider as a controllable input and which as a fluctuating output can affect the description of the system, even though the two cases may appear basically the same. This is the hallmark of statistical ensemble inequivalence in the description of a system.

We point out that the positive definiteness of the differential compliance in the Gibbs ensemble (f ensemble) is dictated by thermodynamics. No such constraint exists for the differential stiffness in the Helmholtz ensemble (X ensemble). This is discussed in Ref. [56].

In the two- or three-state ℓGC, similar tensile elastic behavior to the four-state case is observed. In all cases, they exhibit similar trends with parameter variations as discussed in the previous Sec. III B.

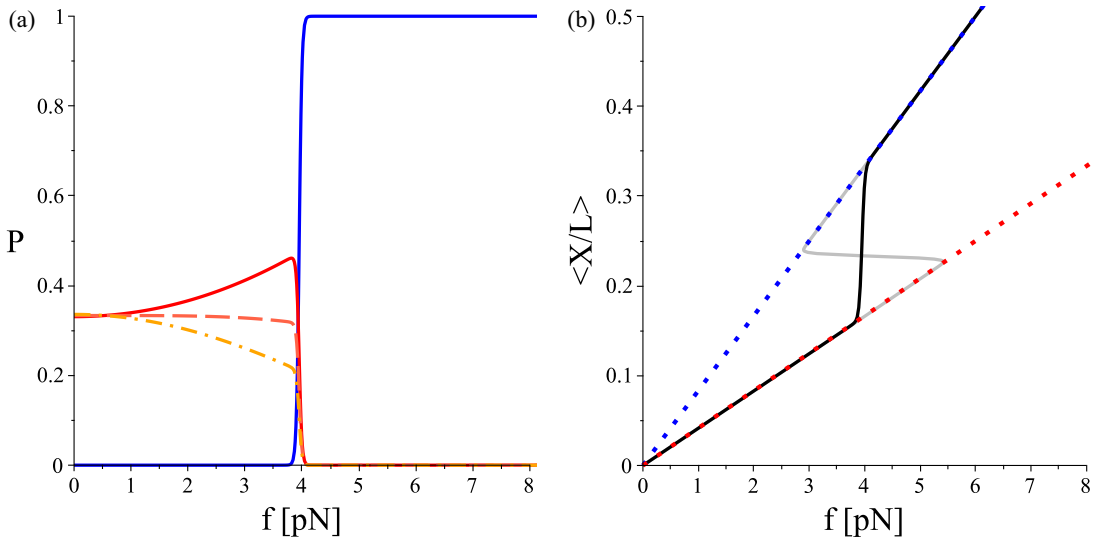

FIG. 3. (a) Probabilities (occurrence frequencies) for each state of the four-state ℓGC in the f ensemble. The red curves correspond to the three looped states: the solid one to the loop consisting of $N + D_0 + D_1$ monomers, the dashed to $N + D_0 + D_2$, and the dash-dotted to $N + D_0 + D_3$. The blue curve corresponds to the unlooped state. (b) The force-extension relation of the four-state ℓGC in the f ensemble (the black curve). For a direct comparison, the inverted force-extension relation of the four-state ℓGC in the X ensemble is displayed together (the gray curve). The dotted lines serve as visual reference, with the red one representing the relation for the single Gaussian loop of $N + D_0 + D_1$ monomers and the blue one for the single Gaussian chain of N monomers.

IV. ZIPPING GAUSSIAN LOOPS

A. Model

The zipping Gaussian loop (zGL) consists of two Gaussian chains forming a closed loop, as illustrated in the left side of Fig. 4. Each of these chains, both upper and lower parts, has the same degree of polymerization N and the same Kuhn length b. The contour length of each part is assumed to remain constant with $L = Nb$. Between the upper and lower parts, a zipping interaction can occur in a one-to-one fashion, where each monomer on one strand binds to a corresponding monomer on the other strand. As we did in the looping Gaussian chain (ℓGC) model, we develop the zipping model by first considering the simplest two-state scenario. In the two-state zGL, we assume that all pairs of monomers are simultaneously zipped or unzipped, akin to breathing. This structure allows the two strands to exist in two distinct states: either the unzipped state (u state), where the strands are separate (unzipped) to form an intact loop, or the zipped state (z state), where the strands are bound (zipped) to form a double-stranded chain. Similar to the looping model [Eq. (12)], we define phenomenological energy parameter ε to account for the zipping interaction as

$$\mathscr{Z}^{\mathrm{G}}_{\mathrm{zGC,z}} = \mathscr{Z}^{\mathrm{G}}_{\mathrm{ds}} \exp\left(\frac{N\varepsilon}{k_{\mathrm{B}}T}\right), \tag{25}$$

where $\mathscr{Z}^{\mathrm{G}}_{\mathrm{zGC,z}}$ is the partition function for the zipped state of the zGC in the f ensemble, $\mathscr{Z}^{\mathrm{G}}_{\mathrm{ds}}$ is the partition function of the double-stranded chain in the f ensemble, and N is the number of bound pairs of monomers. They are to be explained shortly.

When two separate chains bind to become a double-stranded entity, there is a significant increase in its bending stiffness. In order to capture this change, we consider the double-stranded chain in the z state as an equivalent single-stranded chain, characterized by a larger Kuhn length. This is simply realized by introducing an index of stiffening $\gamma > 1$, reflecting the factor by which the Kuhn length increases compared to the one in the u state: $b \to \gamma b$. By the requirement that the total contour length remains constant, the increase in the effective bond length is compensated by the decrease in the number of monomers in the z state: $N \to N/\gamma$.

From this basic two-state construction, we also develop the multistate zGL by allowing partial zipping. This means that it can exist in intermediate states between fully unzipped and fully zipped. In order to rule out the positional degeneracy, we make an assumption that the partial loop (the partially unzipped section) is located in the middle of the zGL, as illustrated in the right side of Fig. 4. The fraction of the number of upper (or lower) monomers that comprise the upper

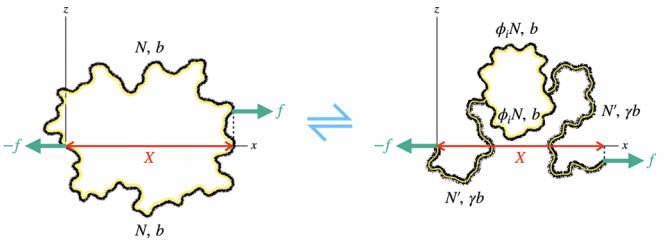

FIG. 4. Model diagram of the zipping Gaussian loop, depicting the unzipped state on the left and a partially zipped state on the right. The partially zipped state consists of a loop (bubble) block at the center, appearing between two zipped blocks. All states of the system maintain the same contour length $L = Nb$, with $N = \phi_i N + 2N'\gamma$. X and $\pm f$ are the control parameters in the extension ensemble and the force ensemble, respectively. The Kuhn length of the zipped blocks is $\gamma b > b$.

(or lower) part of the partial loop in intermediate states is denoted by ϕ ($= n/N$, $n = 1, 2, 3, \ldots$). For parallel discussion with the multistate ℓGC, we extend our exploration of the zGL up to the four-state case. However, unlike the previous narrative, we start our investigation of the zGL with the f ensemble. This choice is motivated by the difficulty involved in constructing the partition function for the intermediate state (partially zipped) within the X ensemble. Here, the control parameter we fix is the total extension of the system, not the sectional extensions. However, the parameters of interest for the construction of the corresponding partition function are precisely these sectional parameters. Furthermore, these sectional extensions fluctuate even within the constraint of fixed total extension. We address this problem by first finding the partition function in the f ensemble and then employing the integral transform relation between the partition functions in the f ensemble and in the X ensemble.

B. Force ensemble

Let us first consider the two-state zGL in the f ensemble. The partition function for the u state is obtained by substituting $N = N_1 = N_2$ into Eq. (7):

$$\mathscr{Z}^{\mathrm{G}}_{\mathrm{zGL,u}} = \left(\frac{3}{4\pi}\right)^{3/2} \tau \zeta^{2N} N^{-3/2} \exp\left(\frac{Nb^2 f^2}{12 {k_\mathrm{B}}^2 T^2}\right). \tag{26}$$

One might think that the partition function for the z state of the equivalent chain [Eq. (25)] could be obtained by substituting $N = N/\gamma$ and $b = \gamma b$ into Eq. (3) with the zipping interaction factor:

$$\begin{aligned}\mathscr{Z}^{\mathrm{G}}_{\mathrm{zGL,z}} &= \mathscr{Z}^{\mathrm{G}}_{\mathrm{ds}} \exp\left(\frac{N\varepsilon}{k_\mathrm{B}T}\right) \\ &= \zeta^{N/\gamma} \exp\left(\frac{(N/\gamma)(\gamma b)^2 f^2}{6 {k_\mathrm{B}}^2 T^2} + \frac{N\varepsilon}{k_\mathrm{B}T}\right).\end{aligned}$$

However, this expression, originating from the single Gaussian chain, loses the intrinsic nature of the loop structure of the zGL, which involves the parameter τ. In order to retain that information, we consider an alternative system for that equivalent chain where just a single pair of monomers forms a loop structure (in a mathematical manner) at one end. Then the partition function for this revised version of the equivalent chain for the z state becomes

$$\begin{aligned}\mathscr{Z}^{\mathrm{G}}_{\mathrm{zGL,z}} &= \zeta^{(N-1)/\gamma} \exp\left(\frac{[(N-1)/\gamma](\gamma b)^2 f^2}{6 {k_\mathrm{B}}^2 T^2} + \frac{(N-1)\varepsilon}{k_\mathrm{B}T}\right)\left(\frac{3}{4\pi}\right)^{3/2} \tau \zeta^2 \exp\left(\frac{b^2 f^2}{12 {k_\mathrm{B}}^2 T^2}\right) \\ &= \left(\frac{3}{4\pi}\right)^{3/2} \tau \zeta^{2+(N-1)/\gamma} \exp\left(\frac{[1+2(N-1)\gamma] b^2 f^2}{12 {k_\mathrm{B}}^2 T^2} + \frac{(N-1)\varepsilon}{k_\mathrm{B}T}\right).\end{aligned} \tag{27}$$

In the multistate zGL, we refer to the intermediate states as z_i state ($i = 2, 3, 4, \ldots$) with the z_1 state being the fully zipped state (the z state in the two-state case). For the intermediate states, we obtain the partition function in the f ensemble

$$\begin{aligned}\mathscr{Z}^{\mathrm{G}}_{\mathrm{zGL},\mathrm{z}_i} &= \zeta^{(1-\phi_i)N/\gamma} \exp\left(\frac{[(1-\phi_i)N/\gamma](\gamma b)^2 f^2}{6 {k_\mathrm{B}}^2 T^2} + \frac{(1-\phi_i)N\varepsilon}{k_\mathrm{B}T}\right)\left(\frac{3}{4\pi}\right)^{3/2} \tau \zeta^{2\phi_i N} (\phi_i N)^{-3/2} \exp\left(\frac{\phi_i N b^2 f^2}{12 {k_\mathrm{B}}^2 T^2}\right) \\ &= \left(\frac{3}{4\pi}\right)^{3/2} \tau \zeta^{[2\phi_i + (1-\phi_i)/\gamma]N} (\phi_i N)^{-3/2} \exp\left(\frac{[\phi_i + 2(1-\phi_i)\gamma] N b^2 f^2}{12 {k_\mathrm{B}}^2 T^2} + \frac{(1-\phi_i)N\varepsilon}{k_\mathrm{B}T}\right),\end{aligned} \tag{28}$$

where $1/N < \phi_i < 1$ is the fraction of the number of monomers comprising the upper (or lower) part of the partial loop in the z_i state. Note that, in the limiting cases of $\phi_i = 1$ or $\phi_i = 1/N$, Eq. (28) becomes the expression for the fully unzipped case [Eq. (26)] or for the fully zipped case [Eq. (27)], respectively. Accordingly, we incorporate the limiting values into the above expression and redesignate the fully unzipped state as the z_0 state with $\phi_0 = 1$, instead of calling it the u state. In this way, we can collectively express the partition functions for all states using the single representation.

In general, the partition function for the m-state zGL ($m = 2, 3, 4, \ldots$) in the f ensemble is $\mathscr{Z}^{\mathrm{G}}_{\mathrm{zGL}} = \sum_{i=0}^{m-1} \mathscr{Z}^{\mathrm{G}}_{\mathrm{zGL},\mathrm{z}_i}$ and the Gibbs free energy is $G_{\mathrm{zGL}} = -kT \ln \mathscr{Z}^{\mathrm{G}}_{\mathrm{zGL}}$. The force extension relation of the m-state zGL in the f ensemble is given by

$$\left\langle \frac{X}{L} \right\rangle = \frac{1}{6}\left(\sum_{i=0}^{m-1} [\phi_i + 2(1-\phi_i)\gamma] P^{\mathrm{G}}_{\mathrm{zGL},\mathrm{z}_i}\right) \frac{f}{k_\mathrm{B}T/b}, \tag{29}$$

where $P^{\mathrm{G}}_{\mathrm{zGL},\mathrm{z}_i} = \mathscr{Z}^{\mathrm{G}}_{\mathrm{zGL},\mathrm{z}_i} / \mathscr{Z}^{\mathrm{G}}_{\mathrm{zGL}}$ is the probability of being in the z_i state in the f ensemble. Figure 5 illustrates the equilibrium statistics and tensile elasticity of the multistate zGL with the four-state case. Figure 5(a) shows the probability for each state and Fig. 5(b) shows the resulting force-extension relation. In this model, we set $T = 300$ K and $b = 10$ Å, following the parameters in the ℓGC model. For practical reasons in numerical calculations, we set $N = 100$. Unlike in the ℓGC model, the value of τ is irrelevant to the result. However, the outcome in this model depends on the value of ζ due to the varying total number of monomers in each state. Consequently, we specify its value as $\zeta = 6$. The new parameters introduced in the zGL model are set as $\gamma = 2$ and $(\phi_0, \phi_1, \phi_2, \phi_3) = (1, 1/100, 33/100, 66/100)$ (fully unzipped, fully zipped, and two partially zipped states). In these prescriptions, the four-state zGL exhibits a crossover between the unzipped state and the zipped state approximately within the range 1.6–2.6$k_\mathrm{B}T$ of ε [the shown plots correspond to $\varepsilon = 2.4 k_\mathrm{B}T$ ($\approx$1.4 kcal/mol)]. The probability pattern reveals that the system is predominantly in either the fully unzipped

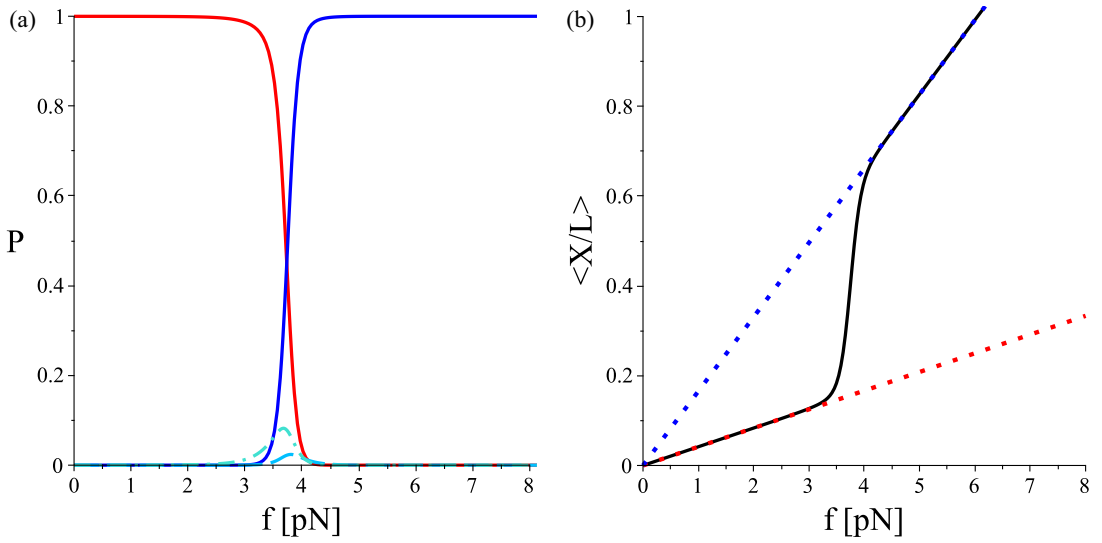

FIG. 5. (a) Probabilities (occurrence frequencies) for each state of the four-state zGL in the f ensemble. The red solid curve corresponds to the fully unzipped state (z_0 state with $\phi_0 = 1$) and the blue solid curve corresponds to the fully zipped (z_1 state with $\phi_1 = 1/N$). The intermediate (partially zipped) states are represented by the dashed curve (z_2 state with $\phi_2 \approx 1/3$) and the dash-dotted curve (z_3 state with $\phi_3 \approx 2/3$). (b) The force-extension relation of the four-state zGL in the f ensemble (the black curve). The dotted lines serve as visual reference, representing the force-extension relations of the single-state zGL: the red one corresponds to the z_0 state and the blue to the z_1 state.

state (z_0 state) at small forces or the fully zipped sate (z_1 state) at large forces. Although the occurrence of the intermediate states (z_2 state and z_3 state) is rare, they have peaks at the transition regime. This all-or-none tendency, either fully zipped or fully unzipped, is reflected in the force-extension relation, resulting in two distinct regimes representing the two dominant states (z_0 state and z_1 state), with the transition regime in between. As in the ℓGC in the f ensemble, the slopes in the force-extension relation of the zGL are always positive.

C. Extension ensemble

In the X ensemble of the zGL, the partition function for the unzipped state ($\phi_0 = 1$) is obtained by substituting $N = N_1 = N_2$ into Eq. (5):

$$\mathcal{Z}^{\mathrm{H}}_{\mathrm{zGL},z_0} = 2\left(\frac{3}{4\pi}\right)^2 \sigma\tau\zeta^{2N} N^{-2} \exp\left(-\frac{3X^2}{Nb^2}\right). \tag{30}$$

For the zipped states—both the fully zipped ($\phi_1 = 1/N$) and the partially zipped ($1/N < \phi_i < 1,\ i = 2, 3, 4, \ldots$) states—finding the partition functions is not straightforward due to the problems outlined earlier in Sec. IV A. Nevertheless, we can determine them inversely from the partition functions in the f ensemble. Let us denote the partition function for the zipped states in the X ensemble as $\mathcal{Z}^{\mathrm{H}}_{\mathrm{zGL},z_i}$. This unknown partition function in the X ensemble and the partition function in the f ensemble, which we have already known, satisfy the relation $\mathcal{Z}^{\mathrm{G}}_{\mathrm{zGL},z_i} = \sum_{\{X\}} \mathcal{Z}^{\mathrm{H}}_{\mathrm{zGL},z_i} \exp(fX/k_{\mathrm{B}}T)$, where $\sum_{\{X\}}$ denotes the sum over all microstates represented by X. We now seek the solution by using an ansatz

$$\mathcal{Z}^{\mathrm{H}}_{\mathrm{zGL},z_i} = A_i \sigma\tau\zeta^{[2\phi_i + (1-\phi_i)/\gamma]N} \times \exp\left(-B_i \frac{X^2}{b^2} + \frac{(1-\phi_i)N\varepsilon}{k_{\mathrm{B}}T}\right),$$

where A_i and B_i are constants to be determined. In the continuum limit of $\sum_{\{X\}} \to \int_{-\infty}^{\infty} dX/\Delta X$, we obtain

$$A_i = 2\left(\frac{3}{4\pi}\right)^2 (\phi_i N)^{-3/2} \{[\phi_i + 2(1-\phi_i)\gamma]N\}^{-1/2},$$

$$B_i = \frac{3}{[\phi_i + 2(1-\phi_i)\gamma]N}.$$

Thus the partition function for the zipped states in the X ensemble is given by

$$\mathcal{Z}^{\mathrm{H}}_{\mathrm{zGL},z_i} = 2\left(\frac{3}{4\pi}\right)^2 \sigma\tau\zeta^{[2\phi_i + (1-\phi_i)/\gamma]N} \times \left\{\phi_i{}^3[\phi_i + 2(1-\phi_i)\gamma]\right\}^{-1/2} N^{-2} \times \exp\left(-\frac{3X^2}{[\phi_i + 2(1-\phi_i)\gamma]Nb^2} + \frac{(1-\phi_i)N\varepsilon}{k_{\mathrm{B}}T}\right). \tag{31}$$

Note that, if $\phi_i = 1$, the above expression yields the result for the unzipped state in Eq. (30). Consequently, by incorporating $i = 0$ into Eq. (31), we can collectively express the partition functions for all states in the X ensemble, as in the f ensemble.

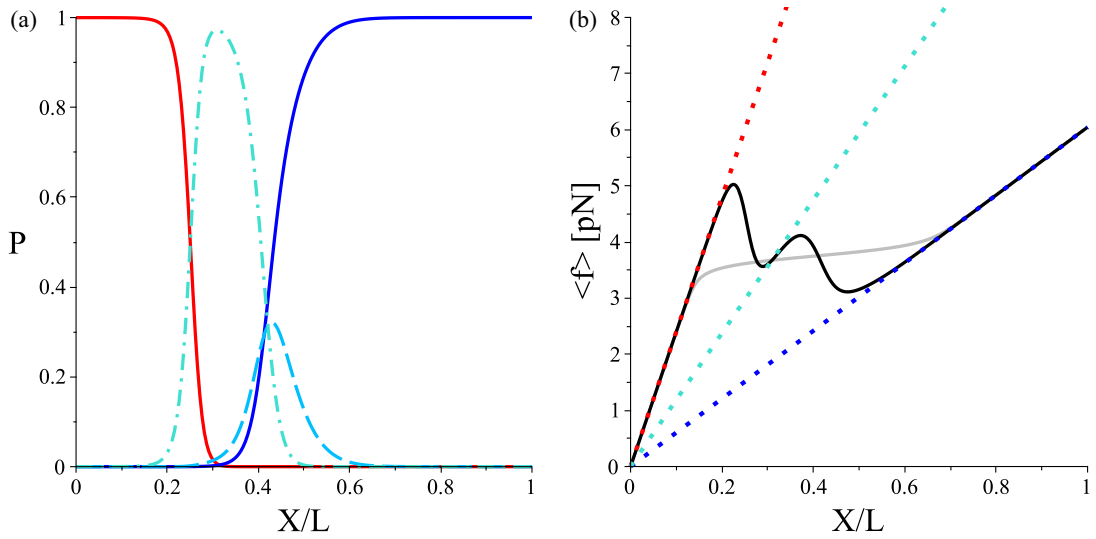

FIG. 6. (a) Probabilities (occurrence frequencies) for each state of the four-state zGL in the X ensemble. The red solid curve corresponds to the fully unzipped state (z_0 state with $\phi_0 = 1$) and the blue solid curve corresponds to the fully zipped (z_1 state with $\phi_1 = 1/N$). The intermediate (partially zipped) states are represented by the dashed curve (z_2 state with $\phi_2 \approx 1/3$) and the dash-dotted curve (z_3 state with $\phi_3 \approx 2/3$). (b) The force-extension relation of the four-state zGL in the X ensemble (the black curve). For a direct comparison, the inverted force-extension relation of the four-state zGL in the f ensemble is displayed together (the gray curve). The dotted lines serve as visual reference, representing the force-extension relations of the single-state zGL: the red corresponds to the z_0 state, the blue to the z_1 state, and the turquoise to the z_3 state. The relation for the z_2 state is not shown.

In general, the partition function for the m-state zGL ($m = 2, 3, 4, \ldots$) in the X ensemble is $\mathscr{Z}^{\rm H}_{\rm zGL} = \sum_{i=0}^{m-1} \mathscr{Z}^{\rm H}_{{\rm zGL},z_i}$ and the Helmholtz free energy is $F_{\rm zGL} = -k_{\rm B}T \ln \mathscr{Z}^{\rm H}_{\rm zGL}$. The force extension relation of the m-state zGL in the X ensemble is given by

$$\left\langle \frac{f}{k_{\rm B}T/b} \right\rangle = 6\left(\sum_{i=0}^{m-1} \frac{1}{\phi_i + 2(1-\phi_i)\gamma} P^{\rm H}_{{\rm zGL},z_i} \right) \frac{X}{L}, \tag{32}$$

where $P^{\rm H}_{{\rm zGL},z_i} = \mathscr{Z}^{\rm H}_{{\rm zGL},z_i} / \mathscr{Z}^{\rm H}_{\rm zGL}$ is the probability of being in the z_i state in the X ensemble. Figure 6 illustrates the behavior of four-state zGL in the X ensemble with the same parameter values as described previously. As in the f ensemble, there is a crossover between the unzipped state and the zipped state. However, the transition regime becomes broader compared to the previous case, as the probabilities of being in the intermediate states (z_2 state and z_3 state) significantly increase. In the case of the z_3 state, where the partial loop accounts for an approximately 2/3 portion ($\phi_3 \approx 2/3$) of the system, its probability peak approaches almost 1, rendering an additional dominance of the z_3 state. This change is reflected in the force-extension relation, resulting in three distinct regimes representing the three dominant states in the order of z_0 state, z_3 state, and z_1 state. Similar to the ℓGC in the X ensemble, the slopes in the two transition regimes between those three regimes are negative, corresponding to a negative extensibility.

In the X ensemble of the four-state zGL, it is possible to develop the suppressed z_2 state with $\phi_2 \approx 1/3$ by adjusting the energy parameter ε. Figure 7 illustrates a variation of Fig. 6 with a change in the value of ε from $2.4k_{\rm B}T$ to $2k_{\rm B}T$. In this modified version, the transition regime becomes much broader as the probabilities of occupying the intermediate states are enhanced. The probability peak of the z_3 state transforms into a plateau of $P = 1$ and the peak of the z_2 state, which was previously low, now reaches a value close to 1. As a result, there are four dominant regimes and three transition regimes between them. Similar phenomena are also observed in the two- and three-state cases, leading to the conclusion that the m-state zGL in the X ensemble can exhibit up to m dominant regimes corresponding to each state or, alternatively, $m - 1$ peaks at maximum in the force-extension relation. This feature, combined with the negative extensibility, constitutes a distinctive characteristic of the X ensemble in the zGL.

V. PHASE TRANSITION IN A GAUSSIAN NECKLACE

We have hitherto focused on the equilibrium statistics and the consequent tensile elastic behavior of the finite-sized systems, where they can reversibly change their overall conformational states. We now expand our exploration by considering the infinitely long Gaussian necklace (GN) with annealed disorder in its local conformational state. This necklace consists of alternating zipped (ordered) and looped (disordered) blocks, concatenated infinitely (Fig. 8). In this thermodynamic limit, we investigate the conformational state of the GN in the presence of a stretching force and its phase diagram in the force-temperature plane.

Our initial step involves constructing the grand partition function, or the generating function, for the GN. The partial grand partition functions for the zipped (labeled as Z) and the

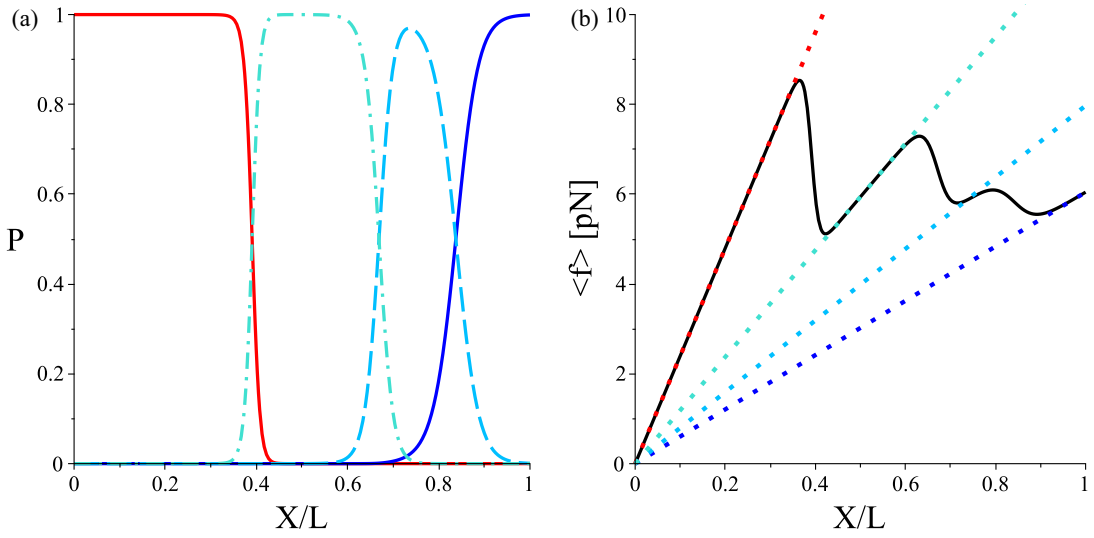

FIG. 7. Modified version of Fig. 6 with a smaller value of ε, while keeping the same values for the other parameters. The transition regime gets broader and three peaks appear in the force-extension relation. The four states are distinguished by the different colors coherently in both plots.

looped (labeled as L) segments are constructed using Eq. (26) and Eq. (27) as

$$\mathscr{G}_{\rm Z}(q) = \sum_{N=1}^{\infty} \mathscr{Z}^{\rm G}_{\rm zGL,z} q^N = \frac{\alpha\Phi q}{1-\Psi q}, \tag{33}$$

$$\mathscr{G}_{\rm L}(q) = \sum_{N=1}^{\infty} \mathscr{Z}^{\rm G}_{\rm zGL,u} q^N = \alpha {\rm Li}_{3/2}(\Phi q), \tag{34}$$

where q is the fugacity for a pair of monomers (one from the upper strand and another from the lower strand), Li is the polylogarithm function, and

$$\alpha = \left(\frac{3}{4\pi}\right)^{3/2} \tau,$$

$$\Phi = \zeta^2 \exp\left(\frac{b^2 f^2}{12 {k_{\rm B}}^2 T^2}\right),$$

$$\Psi = \zeta^{1/\gamma} \exp\left(\frac{\gamma b^2 f^2}{6 {k_{\rm B}}^2 T^2} + \frac{\varepsilon}{k_{\rm B} T}\right).$$

The total grand partition function of the GN is given by

$$\mathscr{G}_{\rm GN}(q) = \sum_{N=1}^{\infty} \mathscr{Z}_{\rm GN} q^N = \frac{\mathscr{G}_{\rm Z}}{1-\mathscr{G}_{\rm Z}\mathscr{G}_{\rm L}}, \tag{35}$$

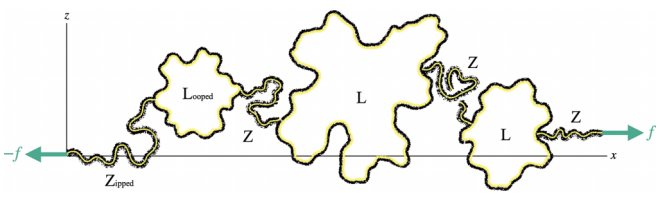

FIG. 8. Model diagram of the Gaussian necklace in the presence of a stretching force ($\pm f$). The zipped and the looped blocks are labeled as Z and L, respectively. In the thermodynamic limit, the two alternate types of blocks are concatenated infinitely as ZLZ $\cdots$ ZLZ.

where $\mathscr{Z}_{\rm GN}$ is the canonical partition function for the GN of N monomer pairs. The free energy density g in the thermodynamic limit is determined by the smallest positive singularity q^* of $\mathscr{G}_{\rm GN}$:

$$g = \lim_{N\to\infty} \frac{-k_{\rm B}T \ \ln \mathscr{Z}_{\rm GN}}{N} = k_{\rm B}T \ \ln q^*. \tag{36}$$

There are three possible candidates for q^*: the smallest positive singularity of $\mathscr{G}_{\rm Z}$, or of $\mathscr{G}_{\rm L}$, or the smallest positive root of the equation

$$\mathscr{G}_{\rm L} = \mathscr{G}_{\rm Z}^{-1}. \tag{37}$$

We note that, in our case, $\mathscr{G}_{\rm L}(q)$ is a monotonically increasing function, starting at (0,0) and ending at $[\Phi^{-1}, \alpha {\rm Li}_{3/2}(1)]$, and $\mathscr{G}_{\rm Z}^{-1}(q)$ is a monotonically decreasing function, starting at $(0, +\infty)$ and passing $(\Psi^{-1}, 0)$. Based on this graphical analysis, we can ascertain the origin of q^*: when $\mathscr{G}_{\rm Z}^{-1}(q)$ at $q = \Phi^{-1}$ is below the critical value

$$\mathscr{G}_{\rm Lc} = \alpha {\rm Li}_{3/2}(1), \tag{38}$$

q^* is given by the root of Eq (37); on the other hand, when $\mathscr{G}_{\rm Z}^{-1}(\Phi^{-1}) > \mathscr{G}_{\rm Lc}$, $q^* = \Phi^{-1}$.

All the thermodynamic properties of the GN are encoded in q^*. Although obtaining an analytic expression of q^* for arbitrary values of the temperature and the stretching force seems unfeasible, its relative position and how it changes with variations in parameters, such as T and f, can still be determined graphically. As T increases from a small value while the other parameters are fixed, $q^*(T)$ increases as the root of Eq. (37), approaching the critical value $q^*(T_{\rm c}) = \Phi^{-1}(T_{\rm c})$, and remains of the form $q^*(T) = \Phi^{-1}(T)$ for $T > T_{\rm c}$ [Fig. 9(a)]. In the case of the f dependence, $q^*(f)$ remains of the form $q^*(f) = \Phi^{-1}(f)$ for $f < f_{\rm c}$ and starts to decrease as the root of Eq. (37) for increasing $f > f_{\rm c}$ [Fig. 9(b)]. The general features of these plots are universal for the necklace model and a pedagogic discussion can be found in Ref. [57].

The observed pattern of $q^*(T, f)$ mirrors the behavior of the free energy density $g(T, f)$ in the thermodynamic limit,

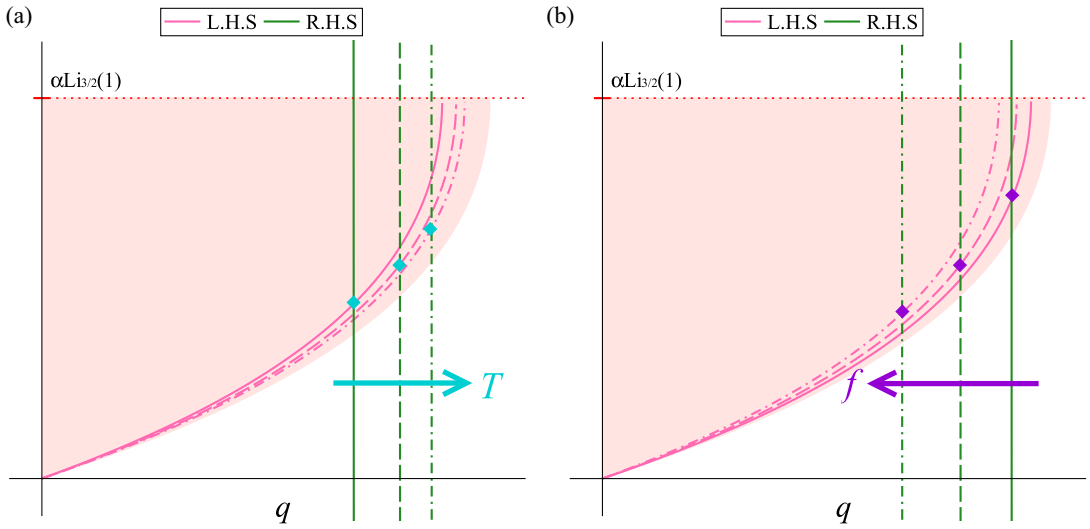

FIG. 9. Plots of $\mathscr{G}_{\rm L}(q)$ [left-hand side (LHS)] and $\mathscr{G}_{\rm Z}^{-1}(q)$ [right-hand side (RHS)] of Eq. (37). We point out that $\mathscr{G}_{\rm Z}^{-1}(q)$ looks like a straight vertical line, whereas in fact it is a curve with a very steep negative slope. (a) $\mathscr{G}_{\rm L}(q)$ and $\mathscr{G}_{\rm Z}^{-1}(q)$ as functions of $q(T)$ with fixed $f = 4$ pN. The solid pair corresponds to $T = 250$ K, the dashed to $T = 300$ K, and the dash-dotted to $T = 350$ K. (**b**) $\mathscr{G}_{\rm L}$ $\mathscr{G}_{\rm Z}^{-1}$ as functions of $q(f)$ with fixed $T = 300$ K. The solid pair corresponds to $f = 3$ pN, the dashed to $f = 4$ pN, and the dash-dotted to $f = 5$ pN. In the both cases, the filled regions represent the area where a solution of $\mathscr{G}_{\rm L}(q) = \mathscr{G}_{\rm Z}^{-1}(q)$ can be found depending on the value of T or f. The red tick marks are the critical value $\alpha{\rm Li}_{3/2}(1)$ of $\mathscr{G}_{\rm L}(q)$ at $q = \Phi^{-1}$. The other setting parameters are $b = 10$ Å, $\zeta = 6$, $\tau = (0.1)^3$, $\gamma = 2$, and $\varepsilon = 2.6 k_{\rm B}T$.

according to Eq. (36). Above the critical temperature $T_{\rm c}$ or below the critical force $f_{\rm c}$, the free energy density always remains of the form $g(T, f) = k_{\rm B}T \ln \Phi^{-1}(T, f)$, which is the one for the infinitely long single loop. On the other hand, below $T_{\rm c}$ or above $f_{\rm c}$, $g(T, f)$ varies differently from $k_{\rm B}T \ln \Phi^{-1}(T, f)$ as q^* switches to the crossing point, which is not given by $\Phi^{-1}(T, f)$, obviously. Since it has lower values than that of the free energy density of the infinite loop, some parts of the necklace must be zipped (bound) for $T < T_{\rm c}$ or $f > f_{\rm c}$. Thus, in terms of the mean fraction of the zipped parts,

$$\langle n_{\rm Z}\rangle = \lim_{N\to\infty}\left\langle \frac{N_{\rm Z}}{N}\right\rangle = \frac{k_{\rm B}T\,\partial \ln q^*}{\partial \varepsilon}, \tag{39}$$

the GN exhibits a phase transition between the mixed state consisting of Z and L blocks ($\langle n_{\rm Z}\rangle \neq 0$) and the completely looped state consisting of a single giant L block ($\langle n_{\rm Z}\rangle = 0$). In principle, if we solve Eq. (37) with respect to q and determine q^*, we can find the mean fraction of the bubbles (looped parts, $1 - \langle n_{\rm Z}\rangle$) as a function of the control parameters of the system in the mixed phase. We can also determine the mean size of a given bubble as

$$\langle N_{\rm L}\rangle = q\frac{\partial \ln \mathscr{G}_{\rm L}}{\partial q} = \frac{{\rm Li}_{1/2}(\Phi q)}{{\rm Li}_{3/2}(\Phi q)} \tag{40}$$

at $q = q^*$. But such an investigation is beyond the scope of this paper.

The order of the transition is a universal property and only depends on the exponent of the power-law dependence of the entropic statistical weight of the looped blocks on their size [45]. It is known that, for an exponent ψ with $1 < \psi < 2$, the transition is continuous. In our case of flexible loops without self-avoidance, the exponent is $3/2$ and thus the phase transition is continuous. The mean fraction of zipped segments plays the role of the order parameter of this phase transition and it goes to zero as we approach the critical point from either below $T_{\rm c}$ or above $f_{\rm c}$.

The critical point $(T_{\rm c}, f_{\rm c})$ satisfies the equation

$$\mathscr{G}_{\rm L}(\Phi^{-1}) = \mathscr{G}_{\rm Z}^{-1}(\Phi^{-1}) \tag{41}$$

and, after some algebra, it yields the equation of phase boundary:

$$(bf_{\rm c})^2 = a(k_{\rm B}T_{\rm c} + u)^2 + w, \tag{42}$$

where

$$\begin{aligned} a &= a(\zeta, \tau, \gamma) \\ &= \frac{12}{\gamma}\ln\zeta + \frac{12}{2\gamma - 1}\ln(1 - c\tau^2), \end{aligned} \tag{43}$$

$$\begin{aligned} u &= u(\zeta, \tau, \gamma, \varepsilon) \\ &= -\frac{\varepsilon}{2(2 - 1/\gamma)\ln\zeta + 2\,\ln(1 - c\tau^2)}, \end{aligned} \tag{44}$$

$$\begin{aligned} w &= w(\zeta, \tau, \gamma, \varepsilon) \\ &= -\frac{3\varepsilon^2}{(2\gamma - 1)[(2 - 1/\gamma)\ln\zeta + \ln(1 - c\tau^2)]}, \end{aligned} \tag{45}$$

and $c = (3/4\pi)^3{\rm Li}_{3/2}(1)$. This equation of the phase boundary implies the phase diagrams that are shown in Fig. 10. Here, we refer to the mixed state as "Bound" and the completely looped state as "Denatured." These terms are borrowed from the melting transition of DNA, even though the GN is not exclusively intended to describe it. When it comes to DNA melting, stretching forces are reported to induce melting [58–61], which is contrary to our result. This discrepancy prompts a comparison with a Poland-Scheraga version of the necklace, as follows.

Let us consider a different type of necklace, denoted by GN′, where the zipped segments of the GN are modeled as

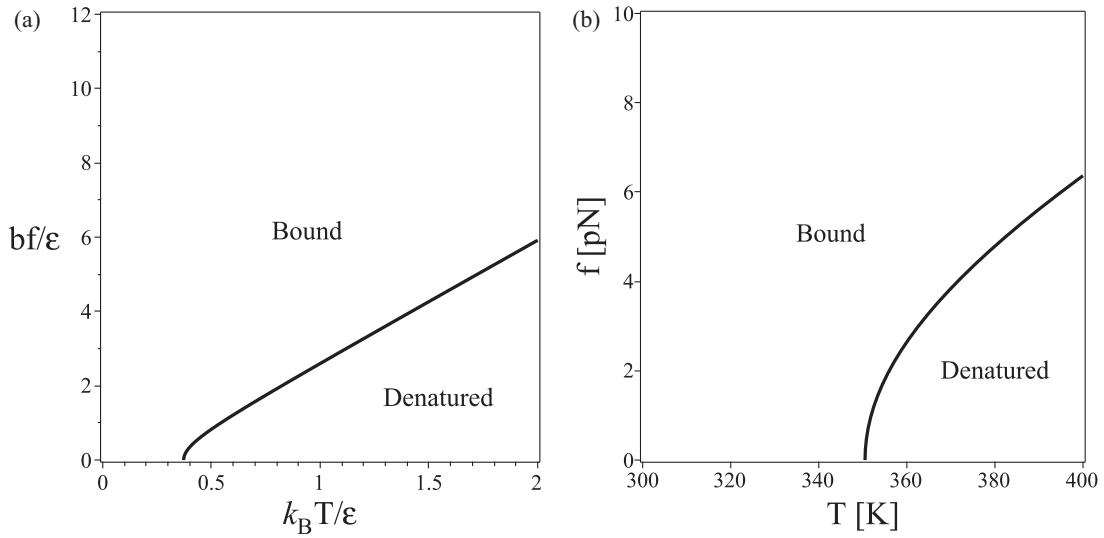

FIG. 10. (a) Phase diagram of the GN in terms of the dimensionless temperature k_BT/ε and the dimensionless force bf/ε. (b) Phase diagram of the GN in terms of the temperature and the force for $b = 10$ Å, $\zeta = 6$, $\tau = (0.1)^3$, $\gamma = 2$, and $\varepsilon = 1.3 \times 10^{-20}$ J (≈1.9 kcal/mol).

rigid rods. The canonical partition function $\mathscr{Z}^{\mathrm{G}}_{\mathrm{zGL,z}}$ in Eq. (33) is then replaced by

$$\mathscr{Z}^{\mathrm{G}}_{\mathrm{R}} = \int d\Omega \, \exp\left(\frac{fNb\cos\theta}{k_BT} + \frac{N\varepsilon}{k_BT}\right) = \frac{4\pi \, \sinh(Nbf/k_BT)}{Nbf/k_BT} \exp\left(\frac{N\varepsilon}{k_BT}\right), \tag{46}$$

where Ω is the solid angle and θ is the polar angle between the rod of length Nb and the axis of the stretching force. Accordingly, the new partial grand partition function for the zipped segment becomes

$$\mathscr{G}'_{\mathrm{Z}} = \sum_{N=1}^{\infty} \mathscr{Z}^{\mathrm{G}}_{\mathrm{R}} q^N = \frac{2\pi k_BT}{bf} \ln\left(\frac{1 - e^{(-bf+\varepsilon)/k_BT} q}{1 - e^{(bf+\varepsilon)/k_BT} q}\right) \tag{47}$$

and the total grand partition function of the GN′ is now given by

$$\mathscr{G}'_{\mathrm{GN}} = \sum_{N=1}^{\infty} \mathscr{Z}'_{\mathrm{GN}} q^N = \frac{\mathscr{G}'_{\mathrm{Z}}}{1 - \mathscr{G}'_{\mathrm{Z}}\mathscr{G}_{\mathrm{L}}}. \tag{48}$$

Because the detailed analysis for the GN′ closely resembles that of the original GN, including the type of the phase transition (continuous), we can now directly jump into the altered equation of phase boundary:

$$\exp\left(\frac{bf_{\mathrm{c}}}{2\pi\alpha \, \mathrm{Li}_{3/2}(1) k_BT_{\mathrm{c}}}\right) = \frac{1 - \zeta^{-2} \exp\left(-\frac{b^2 f_{\mathrm{c}}^2}{12 k_B{}^2 T_{\mathrm{c}}^2} - \frac{bf_{\mathrm{c}}}{k_BT_{\mathrm{c}}} + \frac{\varepsilon}{k_BT_{\mathrm{c}}}\right)}{1 - \zeta^{-2} \exp\left(-\frac{b^2 f_{\mathrm{c}}^2}{12 k_B{}^2 T_{\mathrm{c}}^2} + \frac{bf_{\mathrm{c}}}{k_BT_{\mathrm{c}}} + \frac{\varepsilon}{k_BT_{\mathrm{c}}}\right)}. \tag{49}$$

While this equation cannot be expressed in a closed form like in Eq. (42), it still yields phase diagrams for the GN′ as shown in Fig. 11. Compared to the original case, it exhibits a qualitatively distinct topology in the phase diagram, predicting, under certain conditions, force-induced melting. A reentrance regime appears in the $f - T$ plane, where the phase of the system changes twice with varying values of f or T, eventually returning to the initial phase. It is interesting to point out that the topology of the phase diagram (reentrant transition vs single line) depends on the rigidity of the zipped segments of the model (infinitely stiff vs infinitely flexible).

VI. DISCUSSION AND CONCLUSIONS

The reversible two- or multistate Gaussian loop is the simplest physical system of an unconfined flexible chain that exhibits statistical ensemble inequivalence and negative extensibility in the Helmholtz ensemble. Caruel *et al.* [62,63] have analyzed a mechanical model of the sarcomere cross-bridge, where the cross-bridge is represented by a reversible two-state linear spring. However, the physical realization of that spring is lacking. As far as the pure elasticity is concerned, a (stable) Gaussian chain and a (stable) Gaussian loop are linear springs. An important result of our article is that, in order to properly describe the elasticity of a reversibly looping Gaussian chain (ℓGC), we need to take into account parameters that are commonly ignored when we analyze the stable counterparts (such as the entropy of the dangling ends and the range of the binding potential of the loop). We show that having more than one reversibly looped state (in addition to the open state) does not make any qualitative difference in the elasticity of the system.

In the reversibly zipped Gaussian loop (zGL), we have the whole loop or part of it zipping reversibly. In the zipping process, two linear strands simultaneously and cooperatively bind together. This process has been observed experimentally in the cooperative hybridization of oligonucleotides [38,39]. As in the ℓGC, the reversibly zipped Gaussian loop exhibits statistical ensemble inequivalence and negative extensibility in the Helmholtz ensemble. A significant difference between the elastic behavior of the zGL and that of the ℓGC is the emergence in the latter of a sawtooth pattern with several regions of negative extensibility in the Helmholtz ensemble,

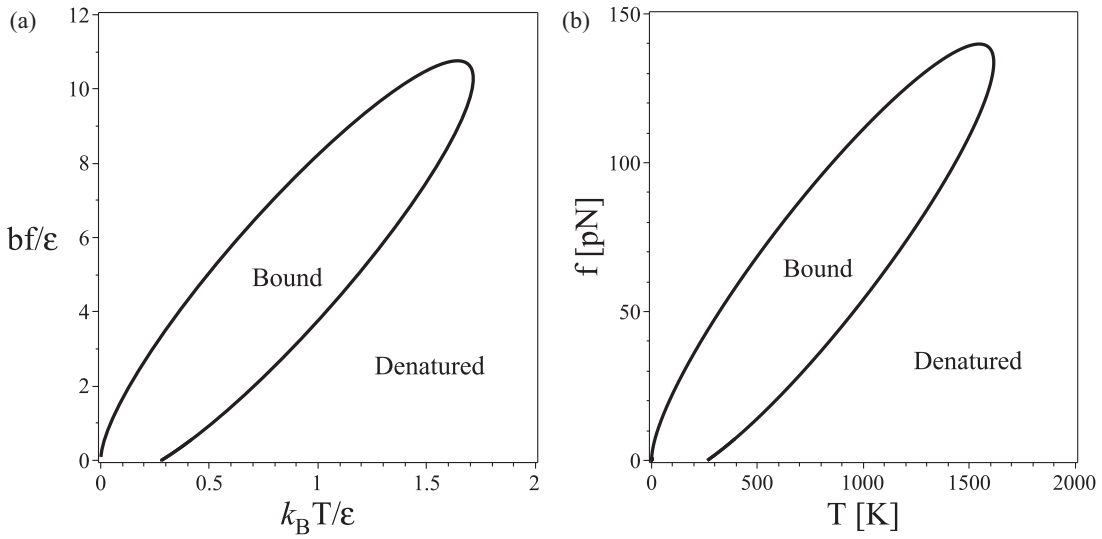

FIG. 11. (a) Phase diagram of the modified version of the Gaussian necklace (GN′) with the zipped blocks represented by rigid rods in terms of the dimensionless temperature k_BT/ε and the dimensionless force bf/ε. (b) Phase diagram of the GN′ in terms of the temperature and the force for the same parameter values as in Fig. 10(b).

if we have multiple zipped states. Giordano *et al.* have shown that flexible chains consisting of bi- or multistable springs also exhibit sawtooth behavior [64–70]. Similar behavior appears in the tensile and bending elasticity of a wormlike chain with bistable blocks (having fluctuating bending stiffness) [56,71].

In this article, we also analyzed the phase behavior of a flexible chain under tension consisting of alternating, reversibly zipped and looped blocks of all possible sizes that we call Gaussian necklace (GN). In our model, both the zipped parts and the looped parts are flexible. The increased stiffness of the zipped blocks is encoded in a larger value of the corresponding Kuhn length. We believe that this approximation is more realistic compared to modeling the zipped blocks as rigid rods. In the thermodynamic limit, the phase behavior is determined by the large-scale conformations of the two types of blocks in the necklace. If we intend to describe chains of contour length much larger than the persistence length, a flexible model for the zipped blocks seems more appropriate. As expected, there is a tension- and temperature-induced continuous phase transition. This is a universal result which depends on the size scaling of the statistical weight of the loops ("bubbles") [45]. An important result of our study is that the phase diagram on the force-temperature plane can have dramatically different form (topology) depending on whether we model the zipped blocks as Gaussian chains or as rigid rods. In our case, the phase boundary between the unzipped and the mixed phase is a curve of positive slope in the $f-T$ plane. If we assume that the zipped parts are rigid rods, the phase boundary becomes a concave curve with a maximum in the same plane. That is the case in the model of Hanke *et al.* who consider self-avoiding flexible loops as bubbles and rigid rods as zipped blocks [47,48].

Our model of the Gaussian necklace is not the first to consider flexible zipped parts, even though it is the simplest and it allows us to obtain an analytic expression for the phase boundary in the $f-T$ plane [Eq. (42)]. Rudnick *et al.* used the generating function method for a self-avoiding necklace whose elements are freely jointed chains [49]. Rahi *et al.* analyzed, using the transfer-matrix method, a necklace whose elements (zipped blocks or looped blocks) consist of small rods connected by aligning hinges [50]. As expected, for small forces, the phase diagrams of those models qualitatively agree with our prediction. There is a discrepancy at higher forces, due to the fact that the Gaussian chain does not satisfy the local inextensibility constraint. The extension of this work to consider freely jointed or wormlike chains, loops, and necklaces is in preparation. We hope to discuss this in detail in a subsequent publication.

ACKNOWLEDGMENTS

This work was supported by a grant from the National Research Foundation of Korea, Grant No. NRF-2022R1F1A1070341, funded by the Ministry of Science and ICT, Korea (MSIT).

[1] R. M. Neumann, Phys. Rev. A **31**, 3516 (1985).
[2] R. M. Neumann, Phys. Rev. A **34**, 3486 (1986).
[3] R. M. Neumann, Biophys. J. **85**, 3418 (2003).
[4] J. T. Titantah, C. Pierleoni, and J.-P. Ryckaert, Phys. Rev. E **60**, 7010 (1999).
[5] M. Süzen, M. Sega, and C. Holm, Phys. Rev. E **79**, 051118 (2009).
[6] R. G. Winkler, Soft Matter **6**, 6183 (2010).
[7] L. I. Klushin, A. M. Skvortsov, and F. A. M. Leermakers, Phys. Rev. E **69**, 061101 (2004).

[8] F. Leermakers, A. Skvortsov, and L. Klushin, J. Stat. Mech.: Theory Exp. (2004) P10001.

[9] A. M. Skvortsov, L. I. Klushin, and F. A. Leermakers, *Macromolecular Symposia* (Wiley Online Library, 2006), Vol. 237, pp. 73–80.

[10] A. Skvortsov, L. Klushin, and F. Leermakers, J. Chem. Phys. **126**, 024905 (2007).

[11] A. Skvortsov, L. Klushin, and T. Birshtein, Polym. Sci. Ser. A **51**, 469 (2009).

[12] S. Dutta and P. Benetatos, Soft Matter **14**, 6857 (2018).

[13] S. Dutta and P. Benetatos, Soft Matter **16**, 2114 (2020).

[14] S. Sinha and J. Samuel, Phys. Rev. E **71**, 021104 (2005).

[15] D. Chaudhuri, Phys. Rev. E **75**, 021803 (2007).

[16] V. Ivanov, L. Klushin, and A. Skvortsov, Polym. Sci. Ser. A **54**, 602 (2012).

[17] R. Schleif, Annu. Rev. Biochem. **61**, 199 (1992).

[18] S. Blumberg, A. V. Tkachenko, and J.-C. Meiners, Biophys. J. **88**, 1692 (2005).

[19] Y.-J. Chen, S. Johnson, P. Mulligan, A. J. Spakowitz, and R. Phillips, Proc. Natl. Acad. Sci. USA **111**, 17396 (2014).

[20] A. A. Shvets and A. B. Kolomeisky, J. Phys. Chem. Lett. **7**, 5022 (2016).

[21] J. Shin and A. B. Kolomeisky, Soft Matter **15**, 5255 (2019).

[22] S. H. Sandholtz, B. G. Beltran, and A. J. Spakowitz, J. Phys. A: Math. Theor. **52**, 434001 (2019).

[23] H. Schiessel, *Biophysics for Beginners: A Journey through the Cell Nucleus* (Jenny Stanford Publishing, Singapore, 2021).

[24] W. Sung, *Statistical Physics for Biological Matter* (Springer, Berlin, 2018).

[25] B. H. Zimm, J. Chem. Phys. **33**, 1349 (1960).

[26] D. Poland and H. A. Scheraga, J. Chem. Phys. **45**, 1464 (1966).

[27] M. Peyrard and A. R. Bishop, Phys. Rev. Lett. **62**, 2755 (1989).

[28] M. Peyrard, Nonlinearity **17**, R1 (2004).

[29] N. Theodorakopoulos, M. Peyrard, and R. S. MacKay, Phys. Rev. Lett. **93**, 258101 (2004).

[30] J. Palmeri, M. Manghi, and N. Destainville, Phys. Rev. E **77**, 011913 (2008).

[31] A.-M. Florescu and M. Joyeux, J. Chem. Phys. **135**, 085105 (2011).

[32] G. Florio, G. Puglisi, and S. Giordano, Phys. Rev. Res. **2**, 033227 (2020).

[33] J. Applequist and V. Damle, J. Am. Chem. Soc. **87**, 1450 (1965).

[34] M. Eigen and D. Pörschke, J. Mol. Biol. **53**, 123 (1970).

[35] F. H. Martin, O. C. Uhlenbeck, and P. Doty, J. Mol. Biol. **57**, 201 (1971).

[36] M. E. Craig, D. M. Crothers, and P. Doty, J. Mol. Biol. **62**, 383 (1971).

[37] M. J. Comstock, T. Ha, and Y. R. Chemla, Nat. Methods **8**, 335 (2011).

[38] K. D. Whitley, M. J. Comstock, and Y. R. Chemla, Nucleic Acids Res. **45**, 547 (2017).

[39] D. Y. Zhang, J. Am. Chem. Soc. **133**, 1077 (2011).

[40] N. F. Dupuis, E. D. Holmstrom, and D. J. Nesbitt, Biophys. J. **105**, 756 (2013).

[41] S. Lifson, J. Chem. Phys. **40**, 3705 (1964).

[42] A. Litan and S. Lifson, J. Chem. Phys. **42**, 2528 (1965).

[43] R.-J. Roe, J. Chem. Phys. **43**, 1591 (1965).

[44] D. Poland and H. A. Scheraga, J. Chem. Phys. **45**, 1456 (1966).

[45] M. E. Fisher, J. Stat. Phys. **34**, 667 (1984).

[46] G. Noh, Two-state semiflexible polymers under tension, Master's thesis, Kyungpook National University, 2021.

[47] A. Hanke, M. G. Ochoa, and R. Metzler, Phys. Rev. Lett. **100**, 018106 (2008).

[48] R. Metzler, T. Ambjörnsson, A. Hanke, and H. C. Fogedby, J. Phys.: Condens. Matter **21**, 034111 (2009).

[49] J. Rudnick and T. Kuriabova, Phys. Rev. E **77**, 051903 (2008).

[50] S. J. Rahi, M. P. Hertzberg, and M. Kardar, Phys. Rev. E **78**, 051910 (2008).

[51] M. Doi, S. F. Edwards, and S. F. Edwards, *The Theory of Polymer Dynamics* (Oxford University Press, Oxford, 1988), Vol. 73.

[52] P.-G. De Gennes, *Scaling Concepts in Polymer Physics* (Cornell University Press, Ithaca, NY, 1979).

[53] M. Rubinstein and R. H. Colby, *Polymer Physics* (Oxford University Press, Oxford, 2003).

[54] A. Y. Grosberg and A. R. Khokhlov, *Statistical Physics of Macromolecules* (Springer, New York, 1994).

[55] K. Huang, *Statistical Mechanics* (John Wiley & Sons, New York, 1987).

[56] P. Benetatos, J. Chem. Phys. **157**, 164112 (2022).

[57] Y. Kafri, D. Mukamel, and L. Peliti, Eur. Phys. J. B **27**, 135 (2002).

[58] I. Rouzina and V. A. Bloomfield, Biophys. J. **80**, 882 (2001).

[59] I. Rouzina and V. A. Bloomfield, Biophys. J. **80**, 894 (2001).

[60] M. Santosh and P. K. Maiti, J. Phys.: Condens. Matter **21**, 034113 (2009).

[61] A. Aggarwal, S. Naskar, A. K. Sahoo, S. Mogurampelly, A. Garai, and P. K. Maiti, Curr. Opin. Struct. Biol. **64**, 42 (2020).

[62] M. Caruel, J.-M. Allain, and L. Truskinovsky, Phys. Rev. Lett. **110**, 248103 (2013).

[63] M. Caruel and L. Truskinovsky, Phys. Rev. E **93**, 062407 (2016).

[64] F. Manca, S. Giordano, P. L. Palla, F. Cleri, and L. Colombo, Phys. Rev. E **87**, 032705 (2013).

[65] F. Manca, S. Giordano, P. L. Palla, and F. Cleri, Physica A **395**, 154 (2014).

[66] S. Giordano, Soft Matter **13**, 6877 (2017).

[67] S. Giordano, Continuum Mech. Thermodyn. **30**, 459 (2018).

[68] M. Benedito and S. Giordano, J. Chem. Phys. **149**, 054901 (2018).

[69] M. Benedito and S. Giordano, Phys. Rev. E **98**, 052146 (2018).

[70] M. Benedito, F. Manca, and S. Giordano, Inventions **4**, 19 (2019).

[71] M. Razbin and P. Benetatos, Polymers **15**, 2307 (2023).